

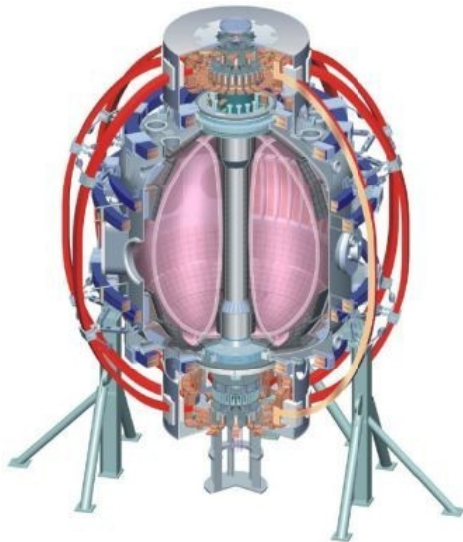
The ME-SXR fast electron temperature diagnostic for NSTX

Kevin Tritz

Johns Hopkins University

D. Clayton, D. Kumar, D. Stutman, M. Finkenthal (JHU)

**53rd annual APS - DPP meeting
Salt Lake City, UT 11/16/2011**



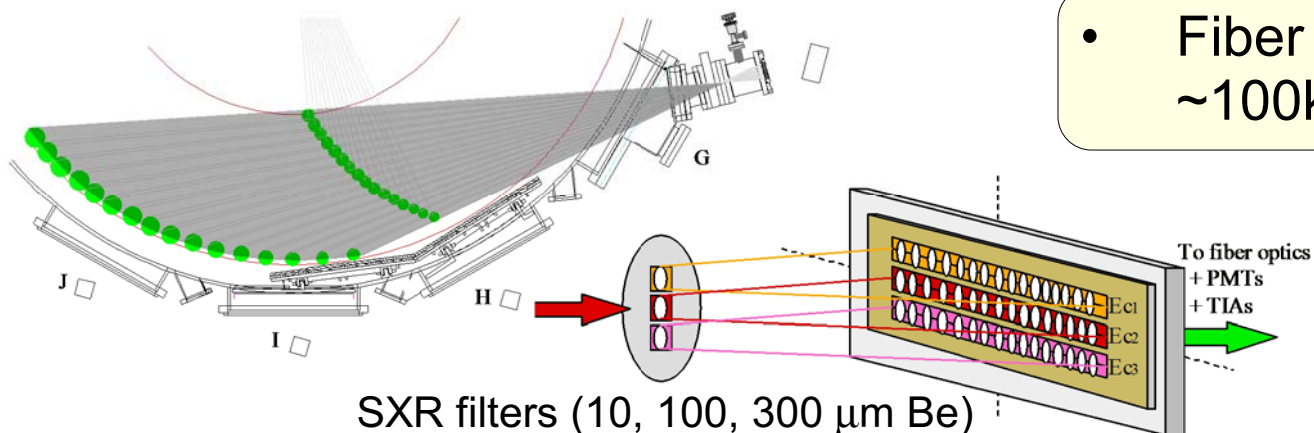
College W&M
Colorado Sch Mines
Columbia U
CompX
General Atomics
INL
Johns Hopkins U
LANL
LLNL
Lodestar
MIT
Nova Photonics
New York U
Old Dominion U
ORNL
PPPL
PSI
Princeton U
Purdue U
SNL
Think Tank, Inc.
UC Davis
UC Irvine
UCLA
UCSD
U Colorado
U Illinois
U Maryland
U Rochester
U Washington
U Wisconsin

Culham Sci Ctr
U St. Andrews
York U
Chubu U
Fukui U
Hiroshima U
Hyogo U
Kyoto U
Kyushu U
Kyushu Tokai U
NIFS
Niigata U
U Tokyo
JAEA
Hebrew U
Ioffe Inst
RRC Kurchatov Inst
TRINITI
KBSI
KAIST
POSTECH
ASIPP
ENEA, Frascati
CEA, Cadarache
IPP, Jülich
IPP, Garching
ASCR, Czech Rep
U Quebec

Viewing the same plasma volume through different filters allows the determination of fast changes in electron temperature, density, and impurity content by comparing the emission from filtered diode arrays.

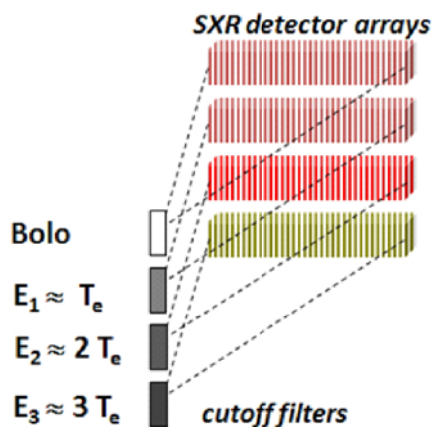
Initial ME-SXR technique used filtered pinhole imaging on a phosphor screen

Multicolor Tangential Optical Soft X-ray Array

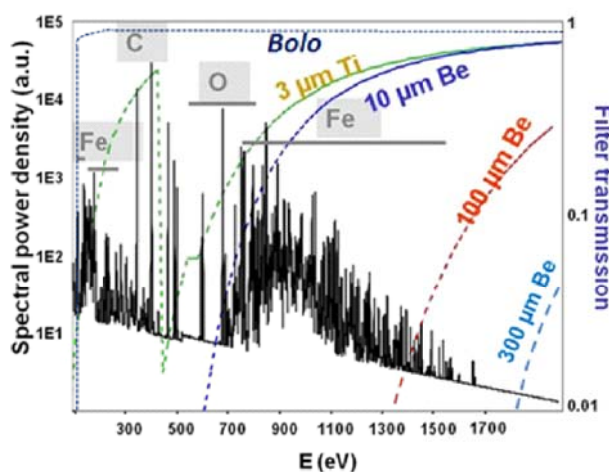


- Fiber coupled to PMTs with $\sim 100\text{kHz}$ time response

SXR filters (10, 100, 300 μm Be)
 Energy_{cutoff} (0.6, 1.6, 2.4 keV)

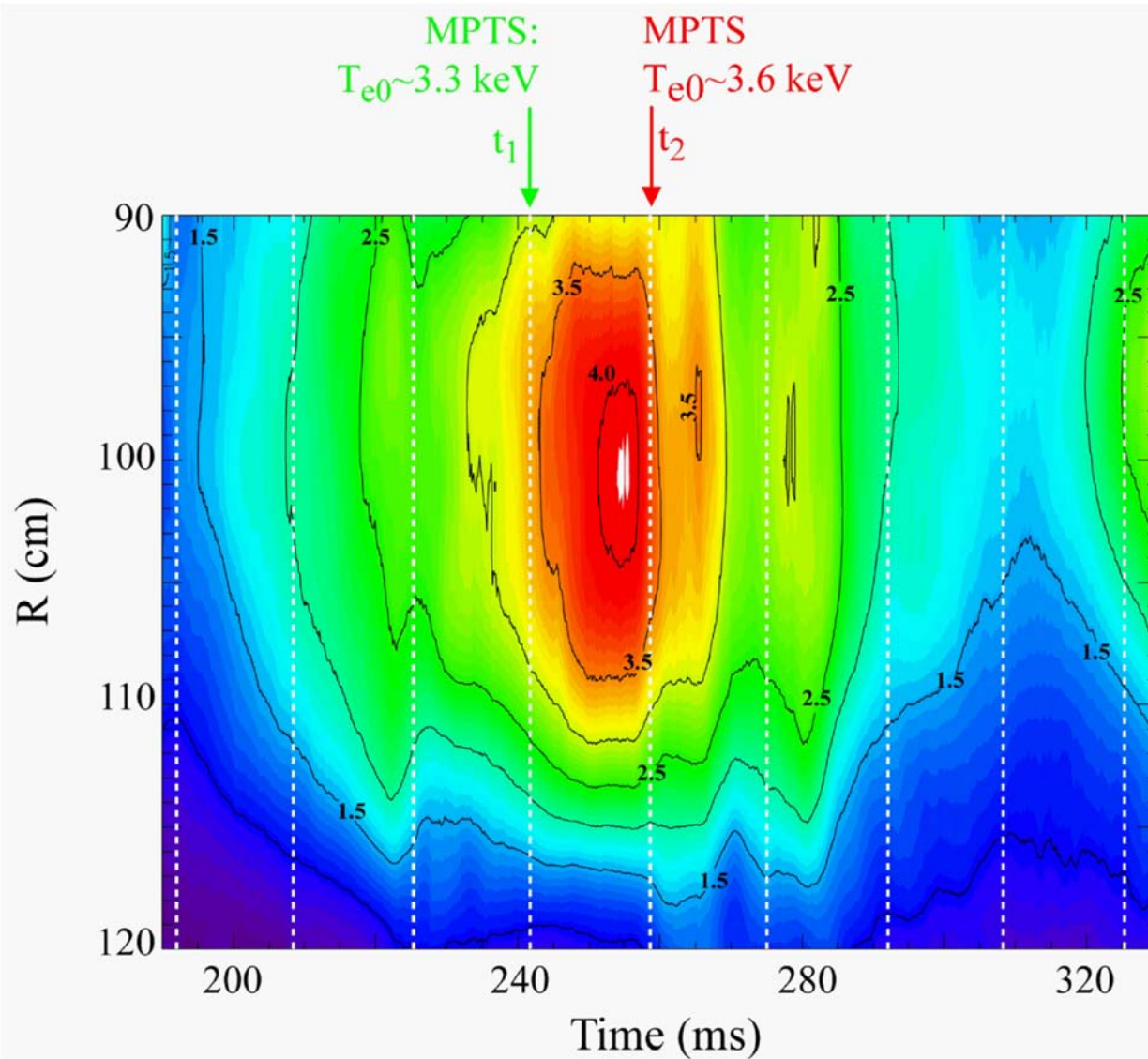


Modeled plasma SXR spectrum



- ME-SXR arrays view same plasma volume through filters with different E_{cutoff}
- Division of SXR spectrum isolates T_e , n_z contribution

ME-SXR fast T_e technique used to reconstruct RF heated T_e profile between MPTS measurements

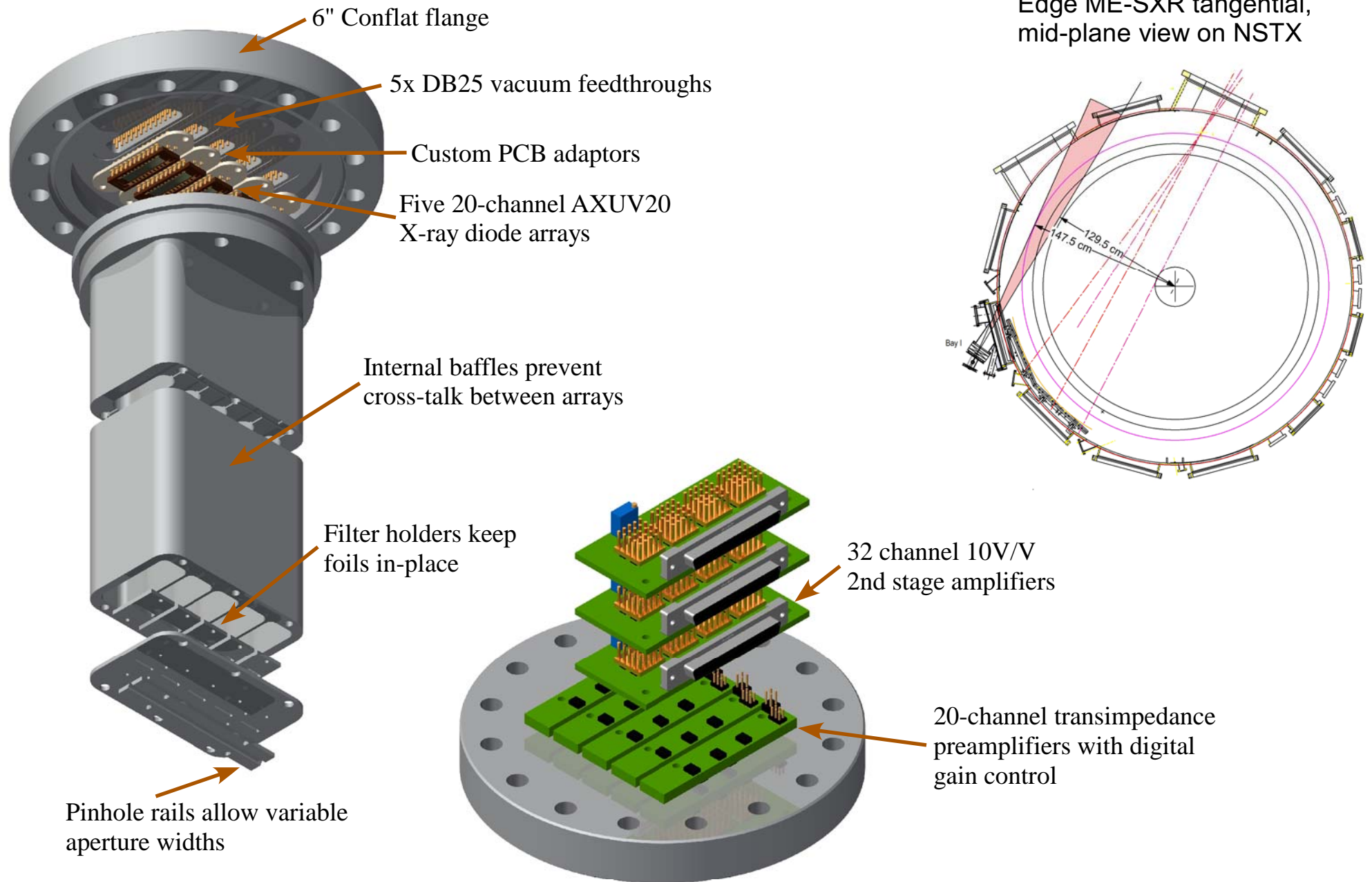


L. Delgado-Aparicio, et al., JAP, **102**, 073304 (2007).

L. Delgado-Aparicio, et al., PPCF, **49**, 1245 (2007).

- Reconstructed T_e shows peak >4 keV, $\sim 15\%$ higher than MPTS measurement
- MPTS profiles used to cross-check ME-SXR reconstruction, provide normalization

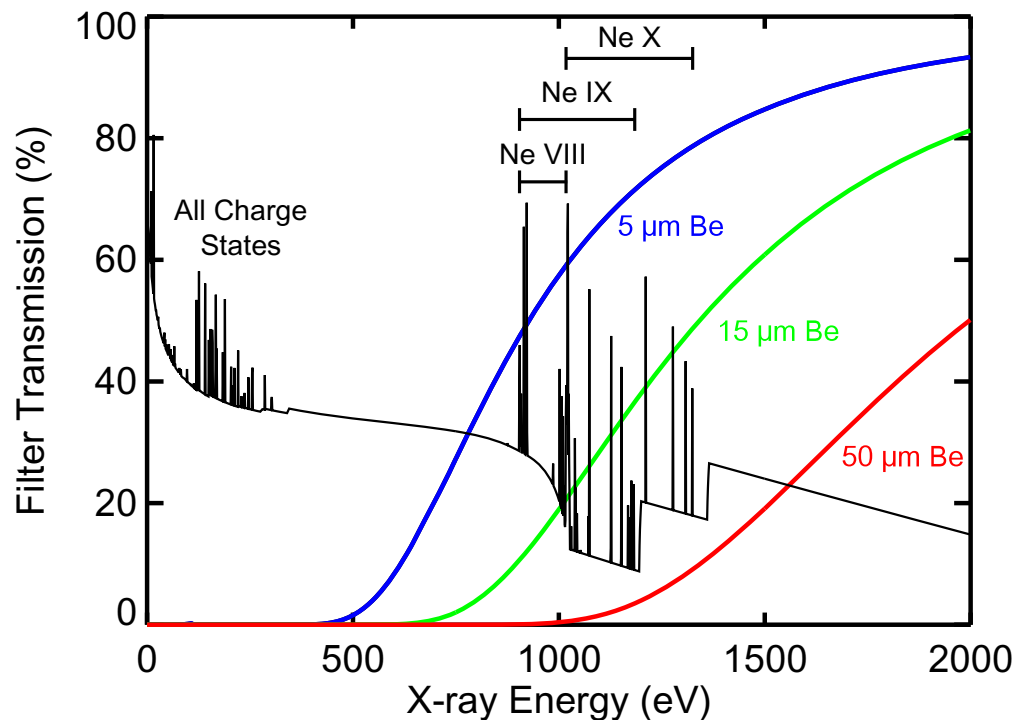
Compact, high-resolution, 5-energy ME-SXR built for ~1cm spatial resolution edge measurements



Different filters provide spectral resolution and variable-gain amplifiers provide good time resolution

- Four arrays have filters (0.3 μm Ti, 5 μm Be, 15 μm Be, 50 μm Be), fifth array is without filter for bolometric measurement
- Pre-amplifiers have digitally controlled variable gains

Modeled plasma SXR spectrum
Neon Emission at 450 eV



Gains	Bandwidth
25 k Ω	300 kHz
100 k Ω	120 kHz
500 k Ω	50 kHz
1 M Ω	35 kHz
2 M Ω	26 kHz
5 M Ω	16 kHz
10 M Ω	11 kHz
20 M Ω	6 kHz

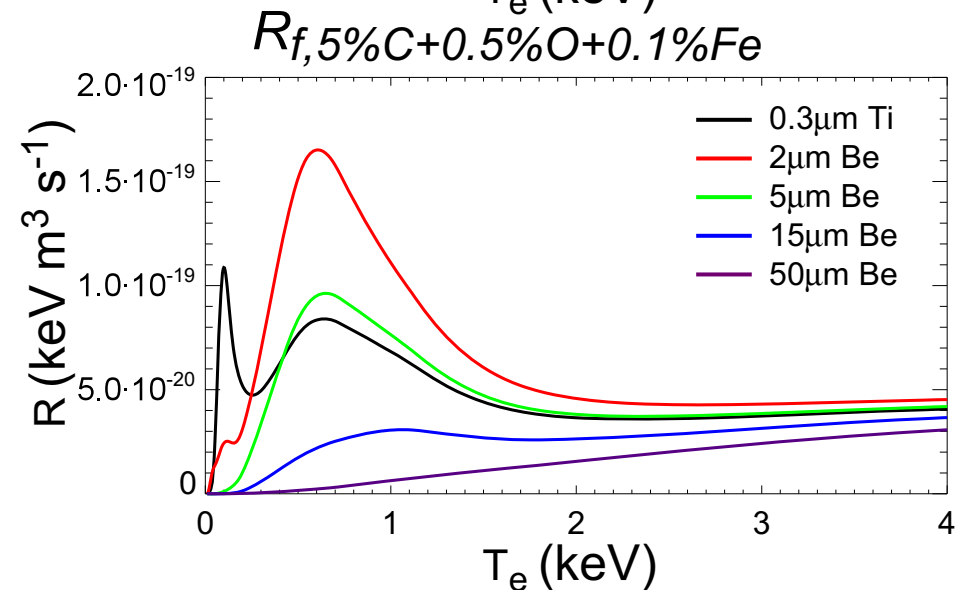
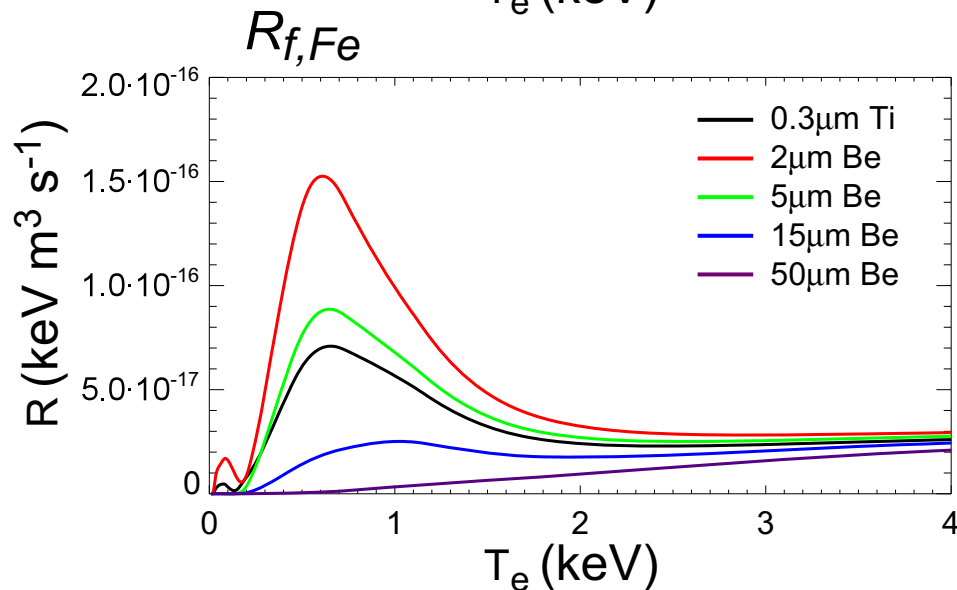
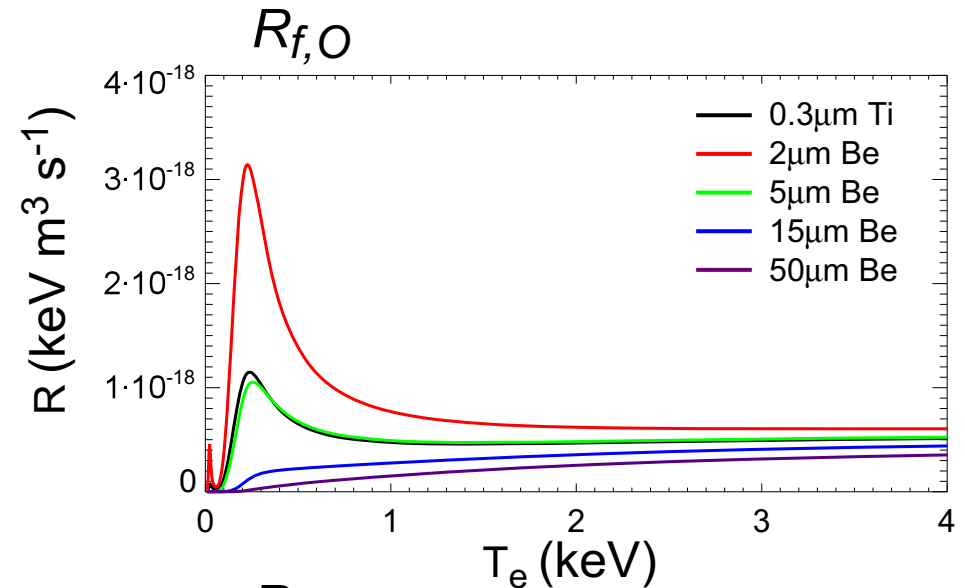
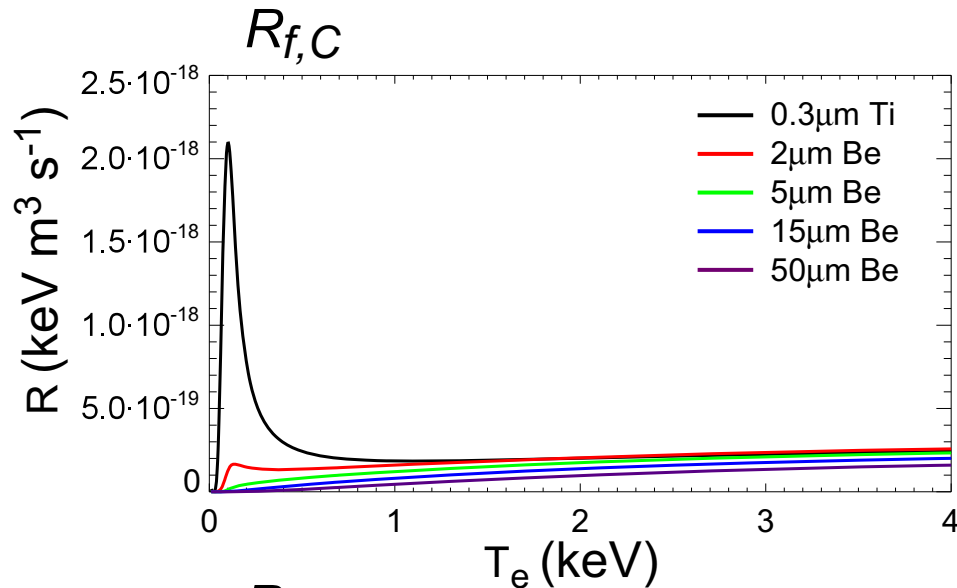
Modeling of ME-SXR Fast T_e : measured X-ray power scales with n_e and T_e -dependent impurity emission

$$\mathcal{E} = n_e \sum_i n_i S_i(T_e, \lambda) = n_e^2 \sum_i c_i S_i(T_e, \lambda) \quad \textcircled{1}$$

$$P_f = \int \mathcal{E} \mathcal{T}_f(\lambda) d\lambda = n_e^2 \sum_i c_i R_{f,i}(T_e) \quad \textcircled{2}$$

- ① Plasma spectral emission function of T_e dependent impurity emission, scales with n_e
- ② SXR detected power measures spectrally integrated product of filter transmission and ①
 - Filtered impurity emission curves $R_{f,i}$ tabulated with spectral modeling codes (e.g. ADAS, CHIANTI)

Spectral modeling codes used to generate filtered impurity response tables



- Different filtered impurity response curves provide ability to isolate temperature sensitivity

Linearized expansion used to isolate SXR emission parametric dependencies

$$\Delta P_f = \frac{\partial P_f}{\partial n_e} \Delta n_e + \frac{\partial^2 P_f}{\partial n_e^2} \frac{\Delta n_e^2}{2} + \frac{\partial P_f}{\partial T_e} \Delta T_e + \frac{\partial^2 P_f}{\partial T_e^2} \frac{\Delta T_e^2}{2} + \frac{\partial^2 P_f}{\partial n_e \partial T_e} \Delta n_e \Delta T_e \quad (3)$$

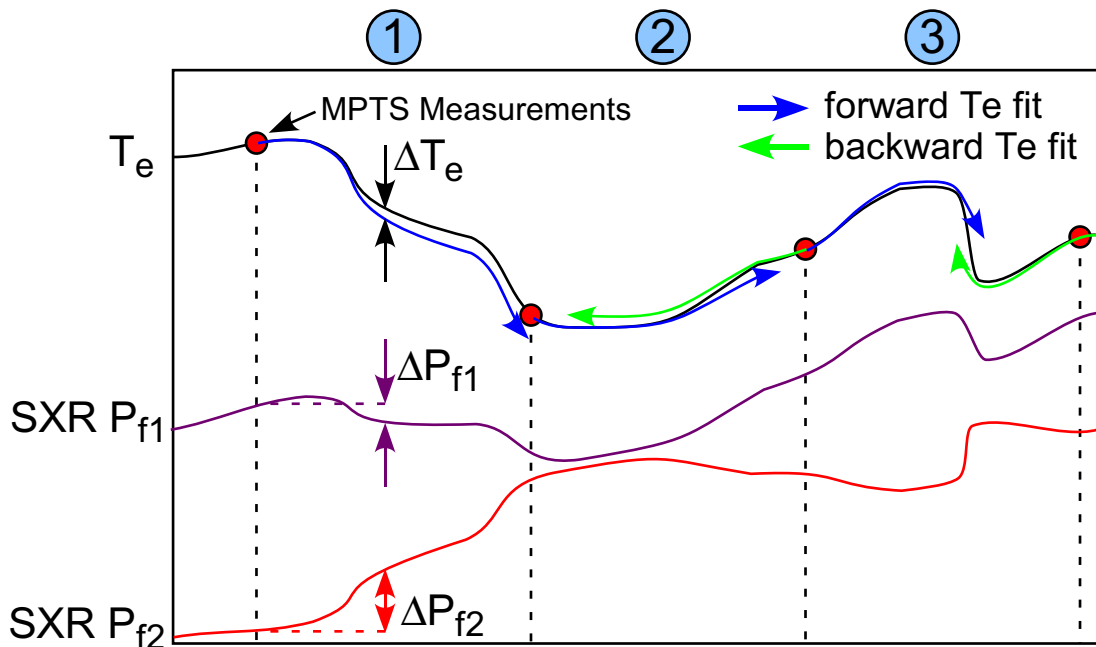
$$\frac{\Delta P_f}{P_f} = \frac{2\Delta n_e}{n_e} + \frac{\Delta n_e^2}{n_e^2} + \frac{\sum_i c_i R'_{f,i}}{\sum_i c_i R_{f,i}} \Delta T_e + \frac{\sum_i c_i R''_{f,i}}{\sum_i c_i R_{f,i}} \frac{\Delta T_e^2}{2} + \frac{2}{n_e} \frac{\sum_i c_i R'_{f,i}}{\sum_i c_i R_{f,i}} \Delta n_e \Delta T_e \quad (4)$$

$$\frac{\Delta P_{f1}}{P_{f1}} - \frac{\Delta P_{f2}}{P_{f2}} = \left(\frac{\sum_i c_i R'_{f1,i}}{\sum_i c_i R_{f1,i}} - \frac{\sum_i c_i R'_{f2,i}}{\sum_i c_i R_{f2,i}} \right) \left(1 + \frac{2\Delta n_e}{n_e} \right) \Delta T_e + \left(\frac{\sum_i c_i R''_{f1,i}}{\sum_i c_i R_{f1,i}} - \frac{\sum_i c_i R''_{f2,i}}{\sum_i c_i R_{f2,i}} \right) \frac{\Delta T_e^2}{2} \quad (5)$$

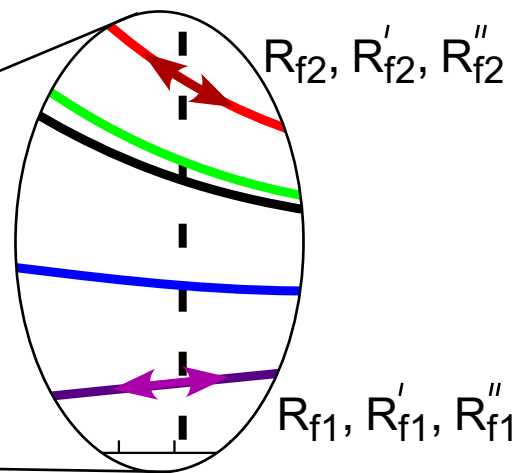
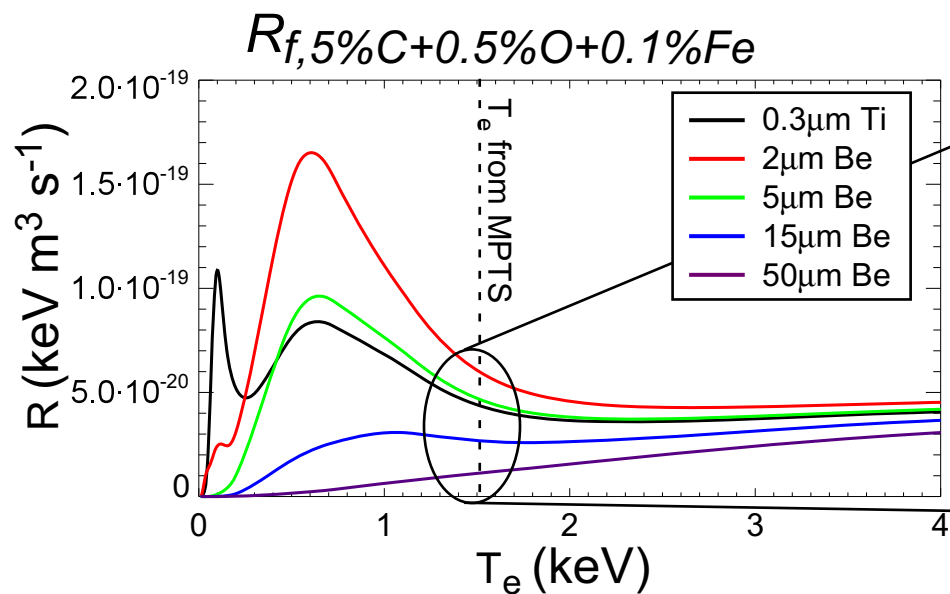
- ③ Linearized Taylor expansion of change in detected power
- ④ Normalized ratio removes need for absolute calibration of detector
- ⑤ Difference of filtered normalized ratio ~isolates T_e , n_e (w/iterations)
 - ΔT_e , Δn_e referenced from intermittent Thomson measurements

ME-SXR measurements of ΔP_f used to propagate fast temperature fits between Thomson measurements

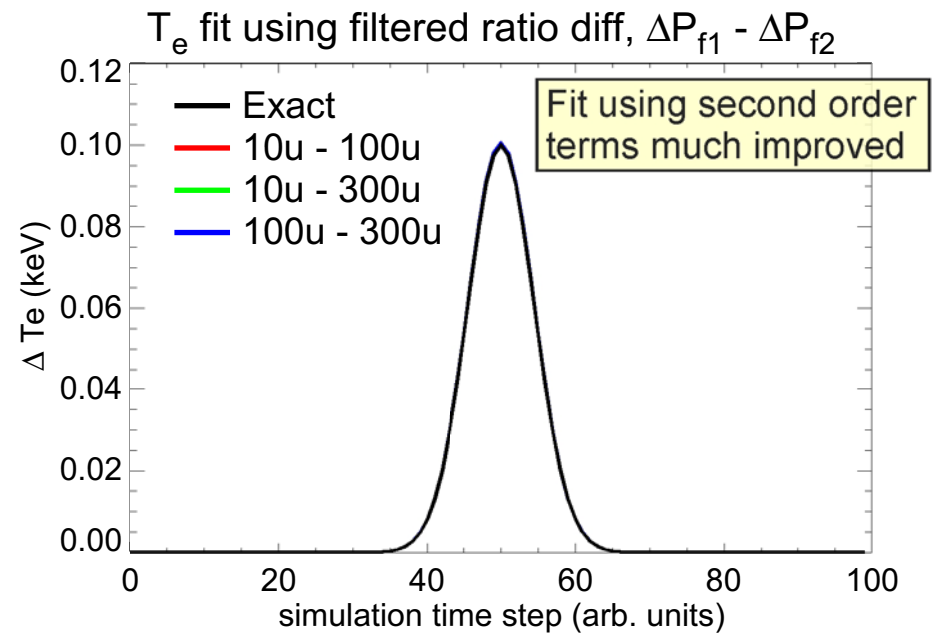
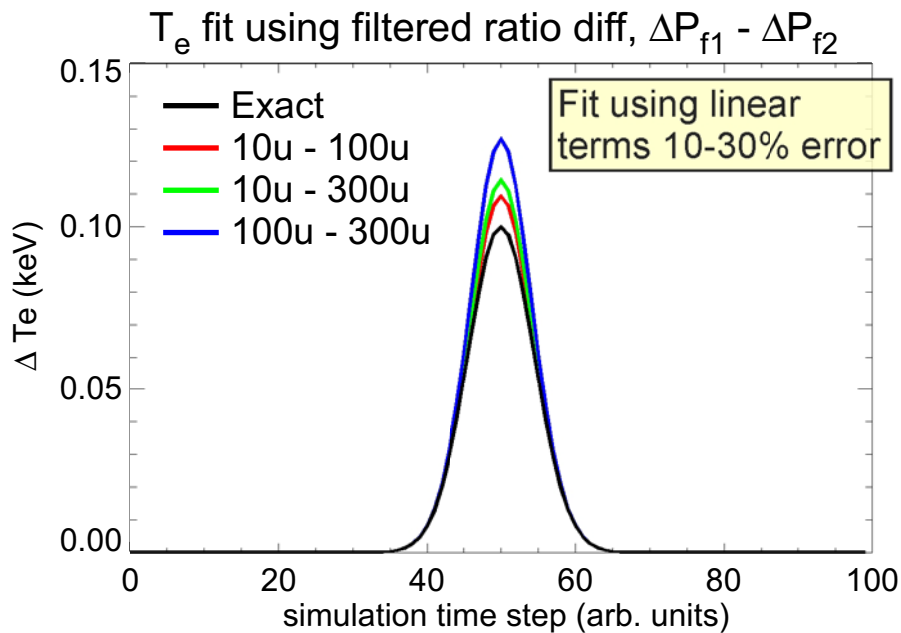
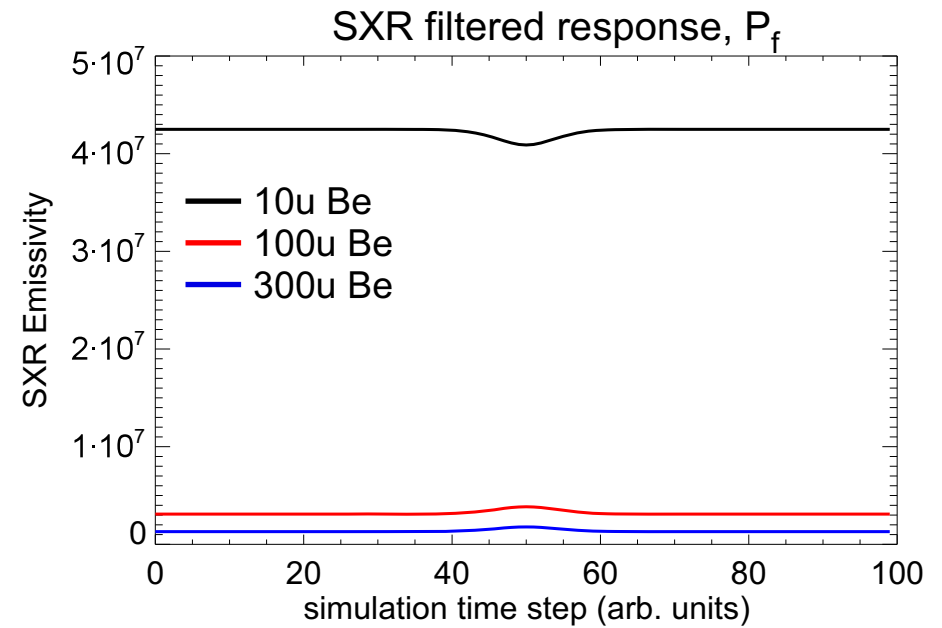
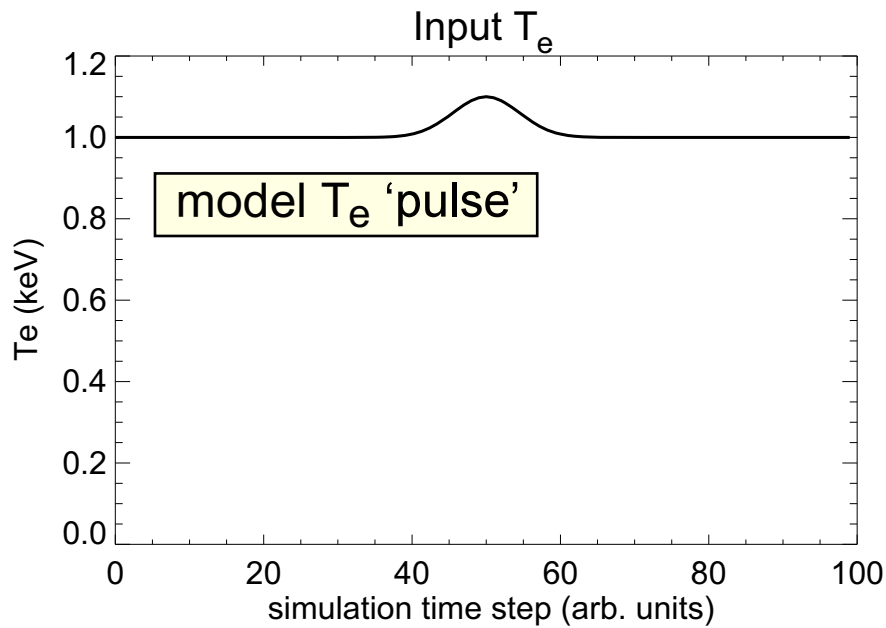
Schematic of ME-SXR fast T_e fitting



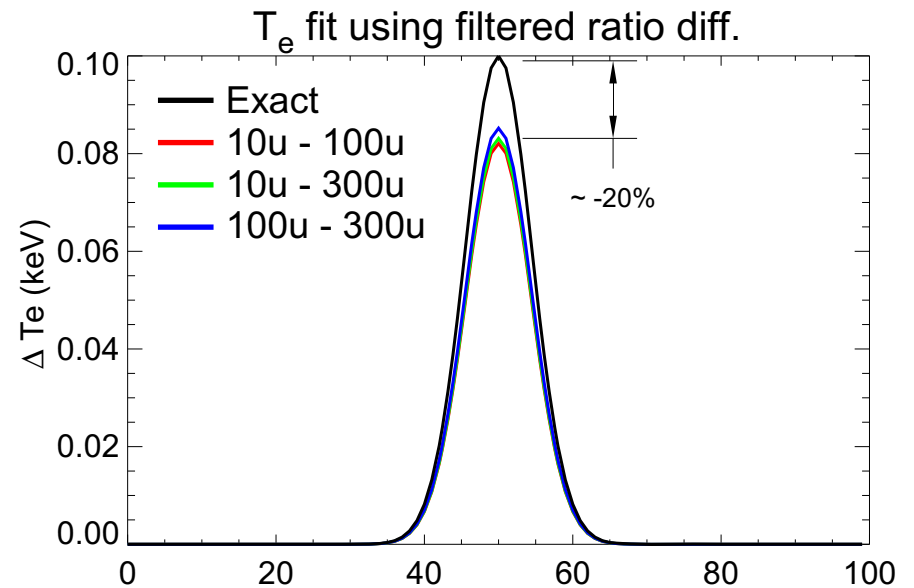
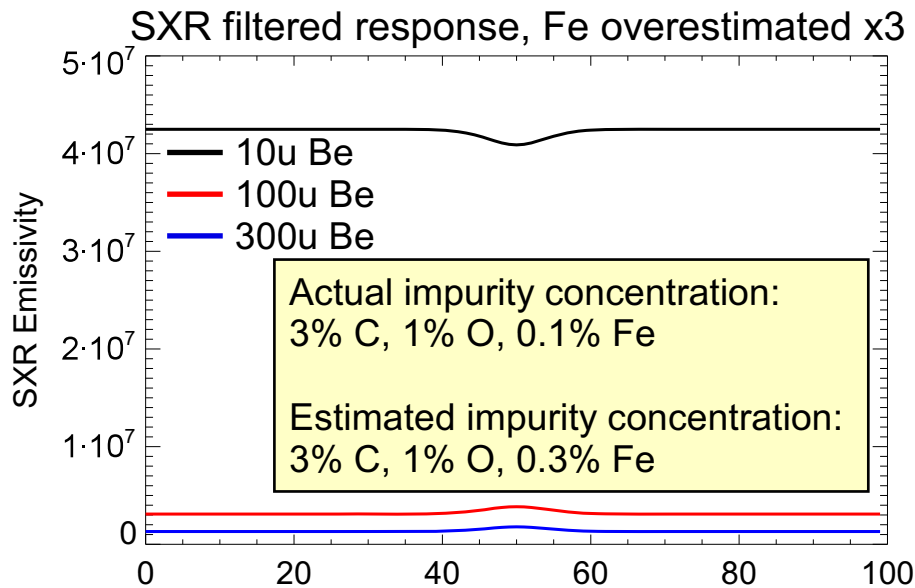
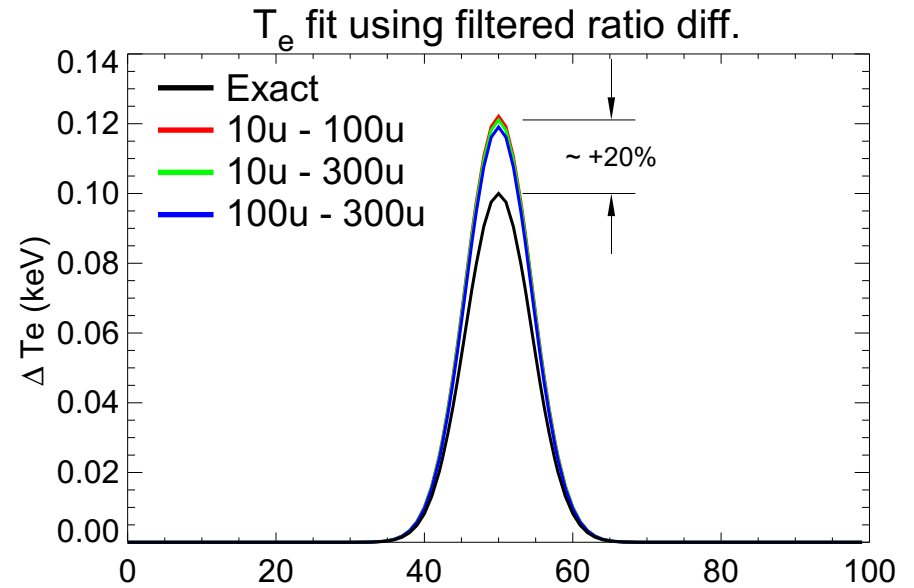
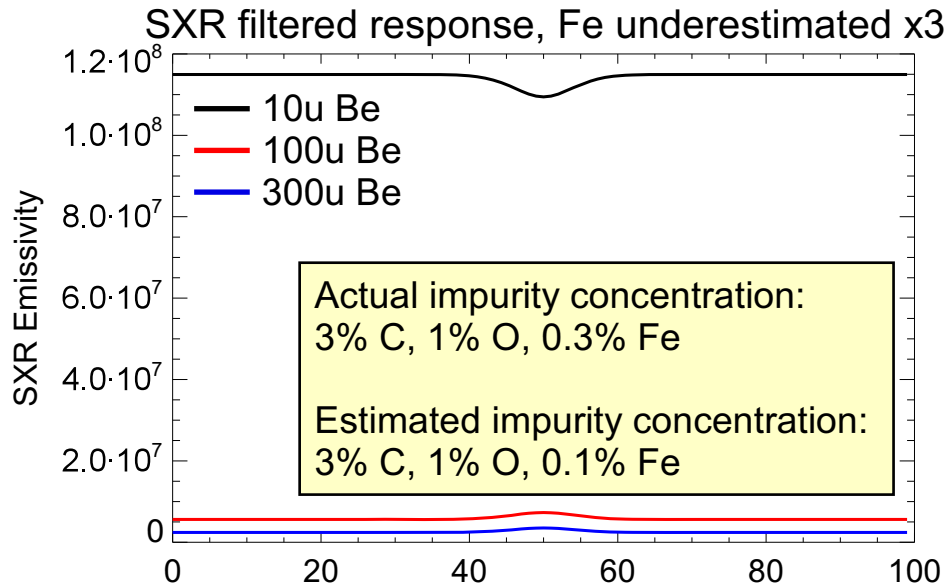
- ① Use MPTS and $R_f(T_e)$ with measured ΔP_f to propagate T_e to next measurement
- ② Compare forward and backward T_e propagation
- ③ Large change in plasma composition may accompany fast T_e changes



2nd-order linearized expansion terms retained to improve ME-SXR fast T_e reconstruction

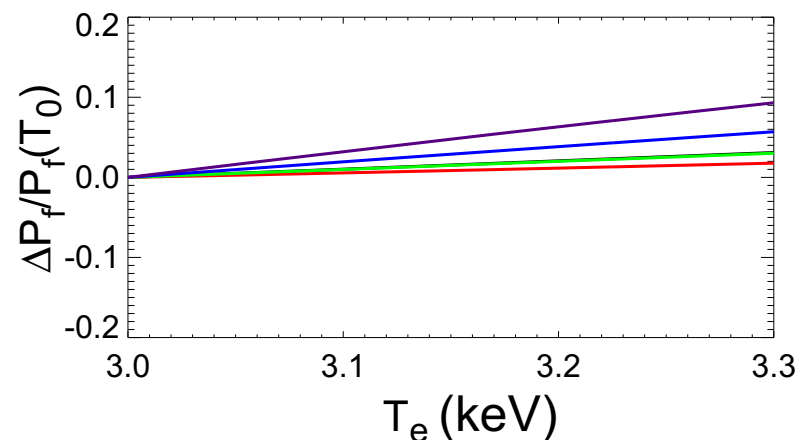
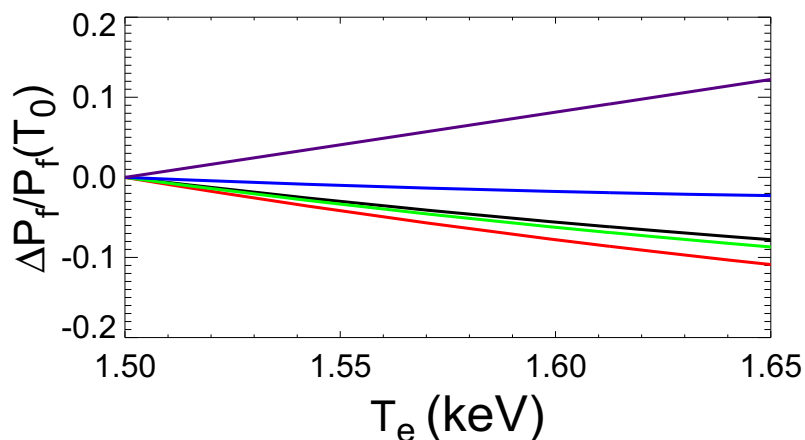
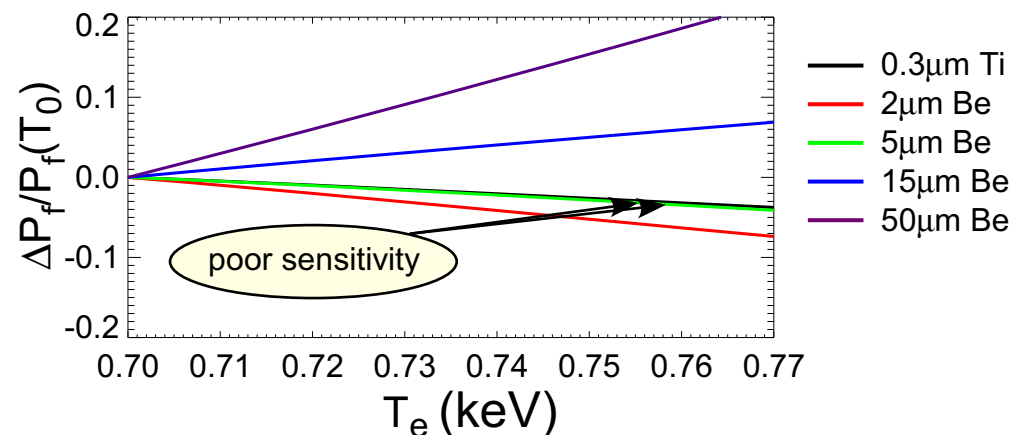
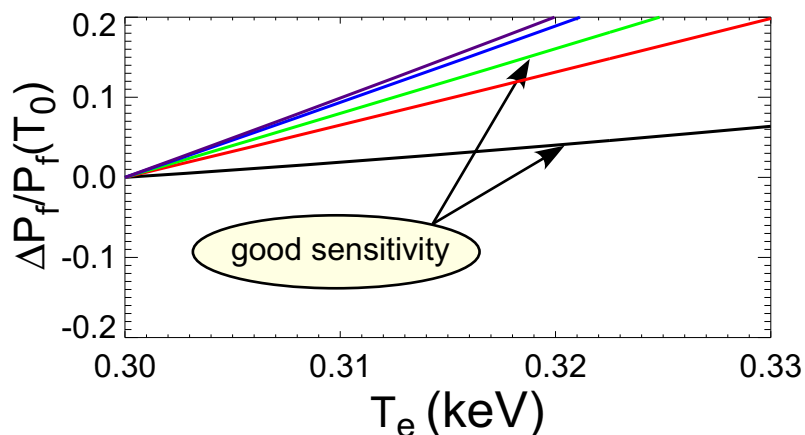


Temperature fits relatively insensitive to uncertainties in impurity concentrations



Filtered material/thickness optimization depends on plasma temperature and impurity content

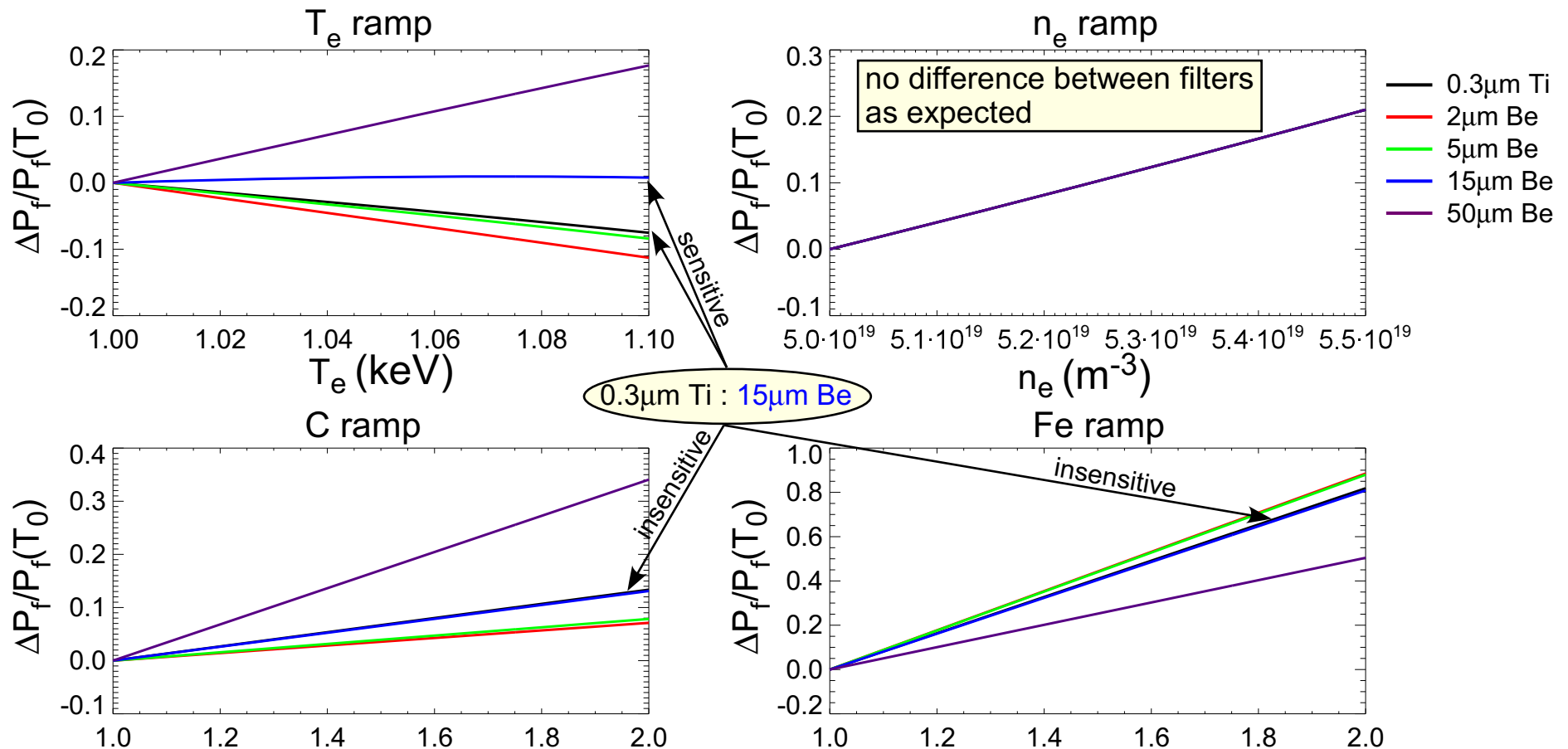
Model SXR response to 10% temperature ramp with plasma impurity content: 5%C, 0.5%O, 0.1%Fe



- 0.3 μm Ti : 5 μm Be filter difference comparison shows good sensitivity at low T_e , loses sensitivity as T_e increases
- Thicker filters improve sensitivity as T_e increases

Multiple filters necessary to discriminate between changes in T_e and changes in impurity fractions

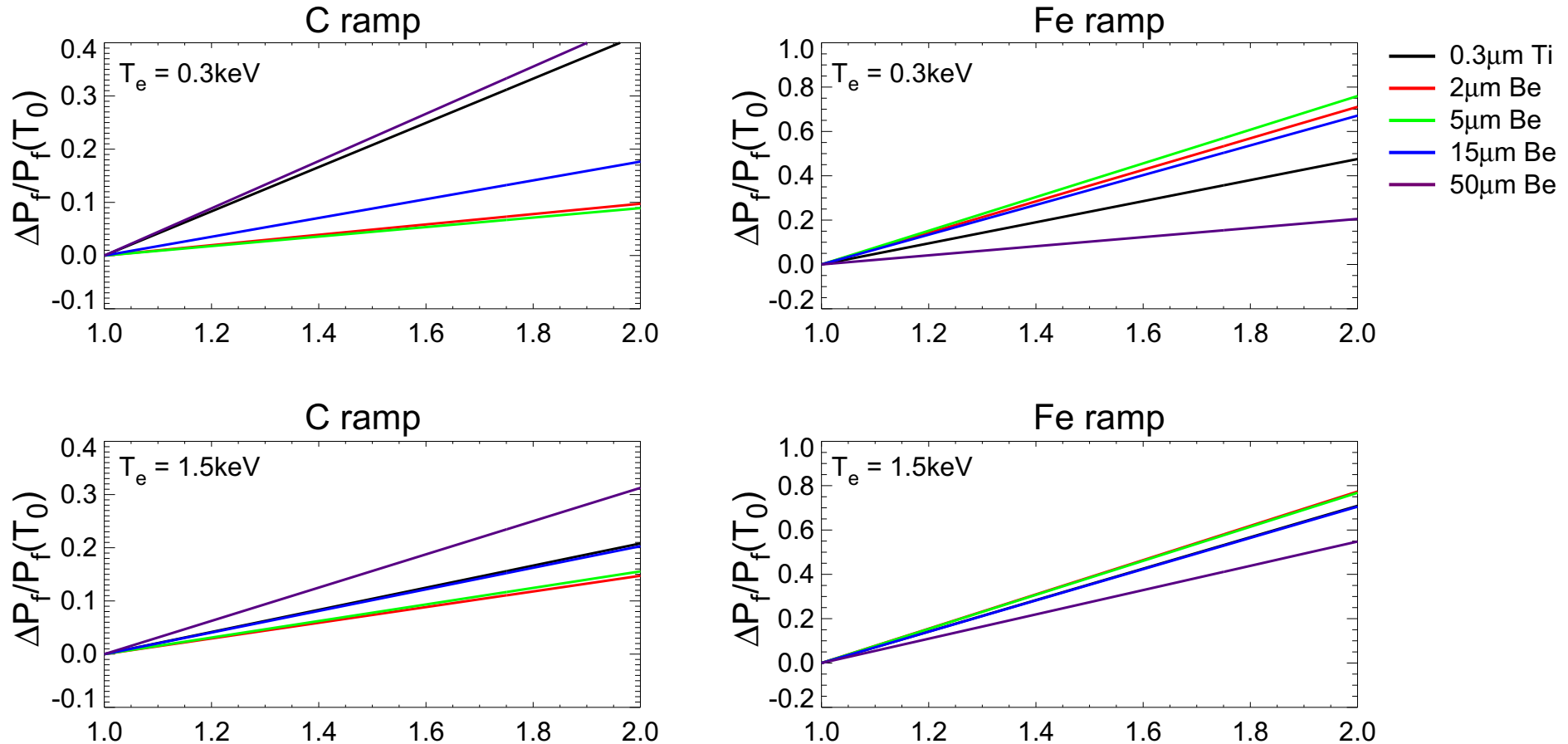
Model SXR response with plasma impurity content: 5%C, 0.5%O, 0.1%Fe



- 0.3 μm Ti : 15 μm Be filter difference insensitive to impurity change, shows good sensitivity to T_e change
- 50 μm filter good candidate to detect impurity change

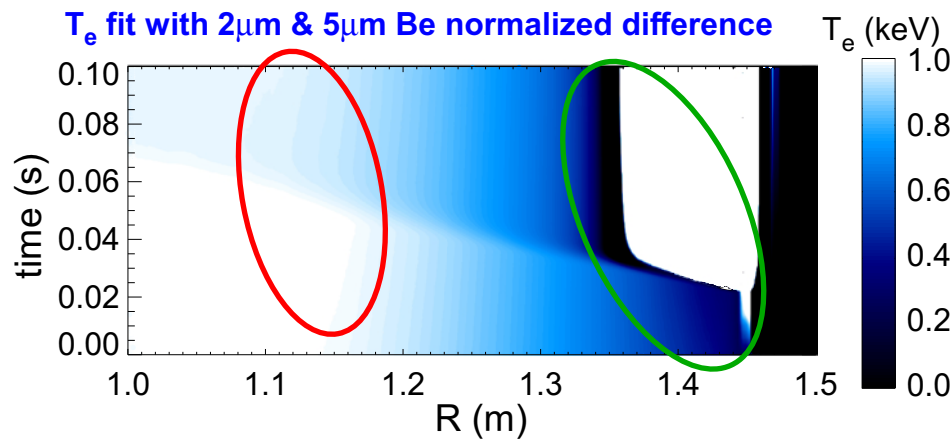
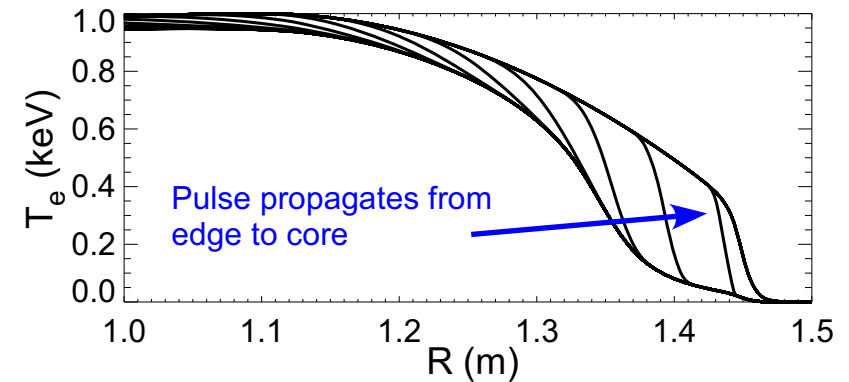
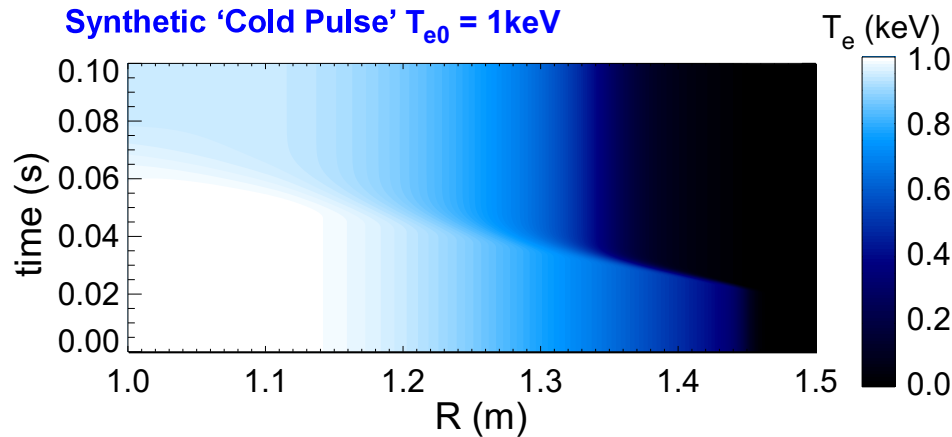
Impurity sensitivity also depends on plasma T_e

Model SXR response with plasma impurity content: 5%C, 0.5%O, 0.1%Fe



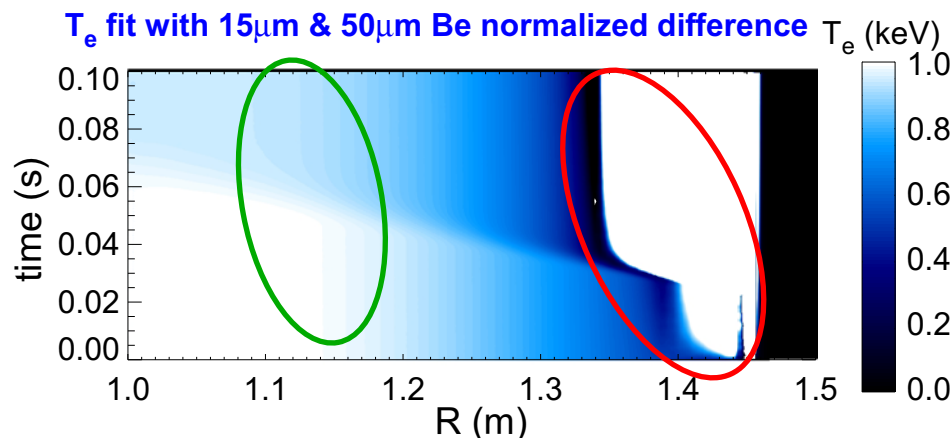
- 0.3 μm Ti filtered SXR response changes sensitivity at low T_e
- Combinations of multiple filters necessary for discrimination of SXR response to ΔT_e and impurity response over range of temperatures

Reconstruction of synthetic 'cold pulse' shows good sensitivity to changes in T_e



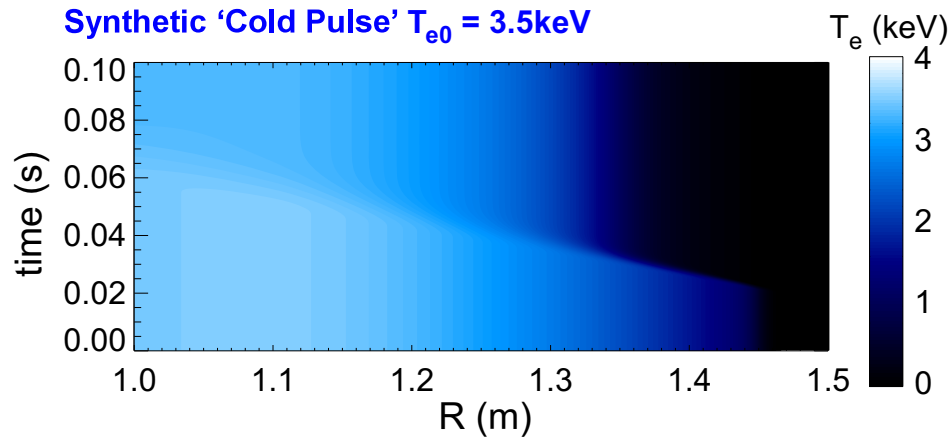
$\text{SNR}_{\text{peak}} \sim 200$

- Thin filters do better at lower T_e reconstruction near edge, overestimate T_e in core

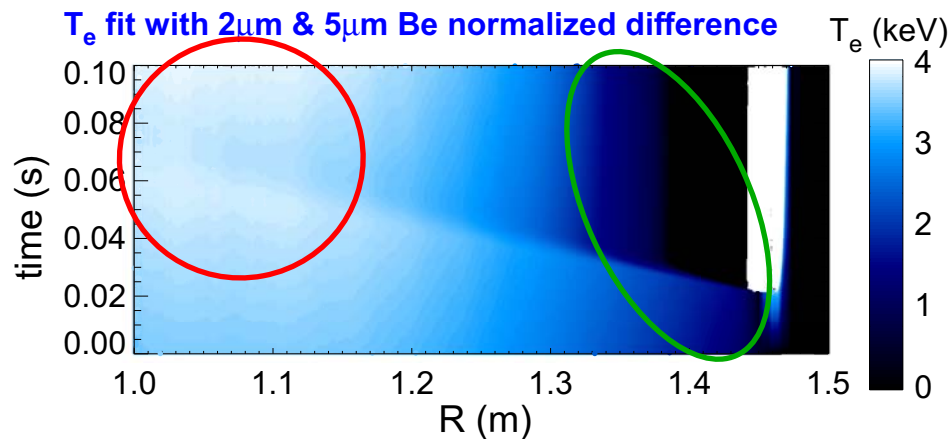


- Thicker filters fit T_e well in core, have difficulty with low signal in edge region

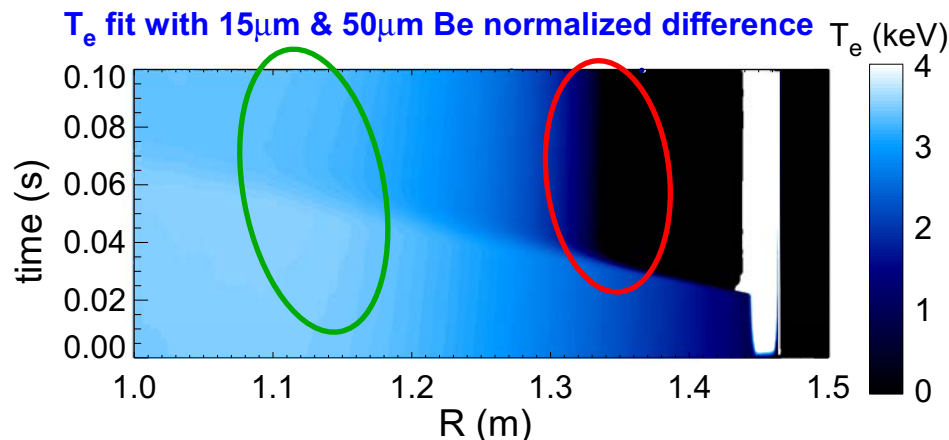
Modeling cold pulse at higher T_{e0} highlights need for multiple filter thicknesses



- Plasma composition same as 1keV model:
5% C, 0.5% O, 0.1% Fe



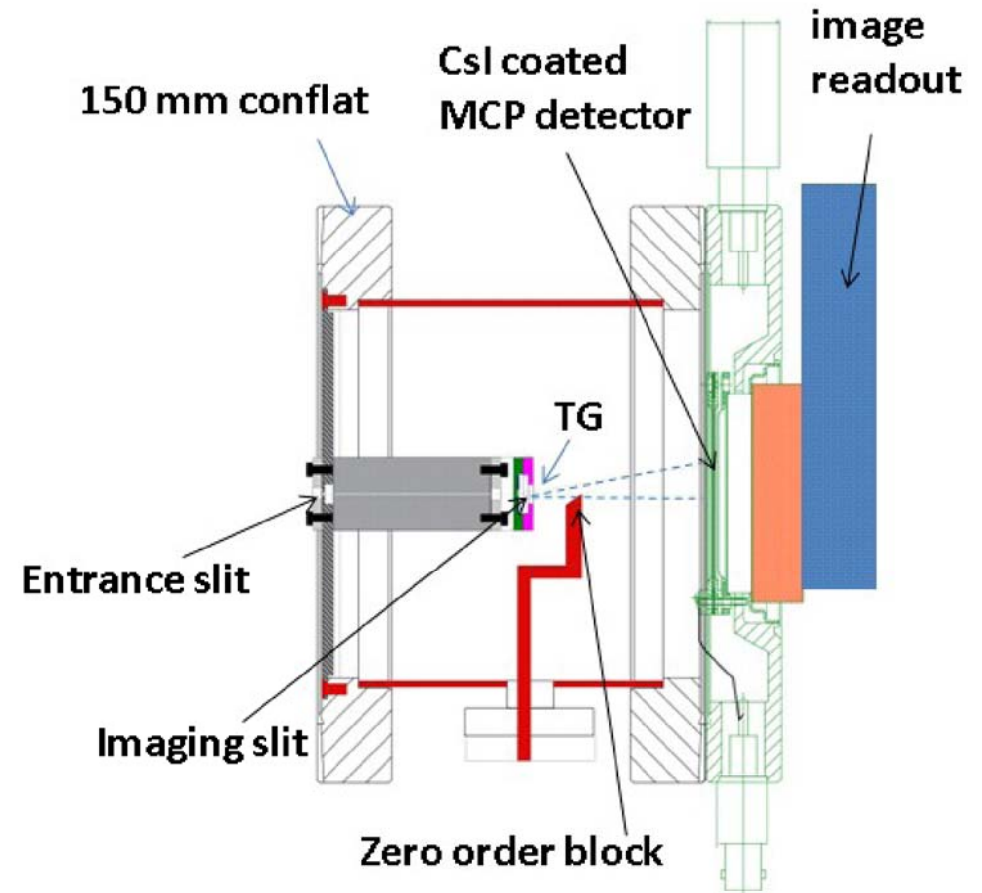
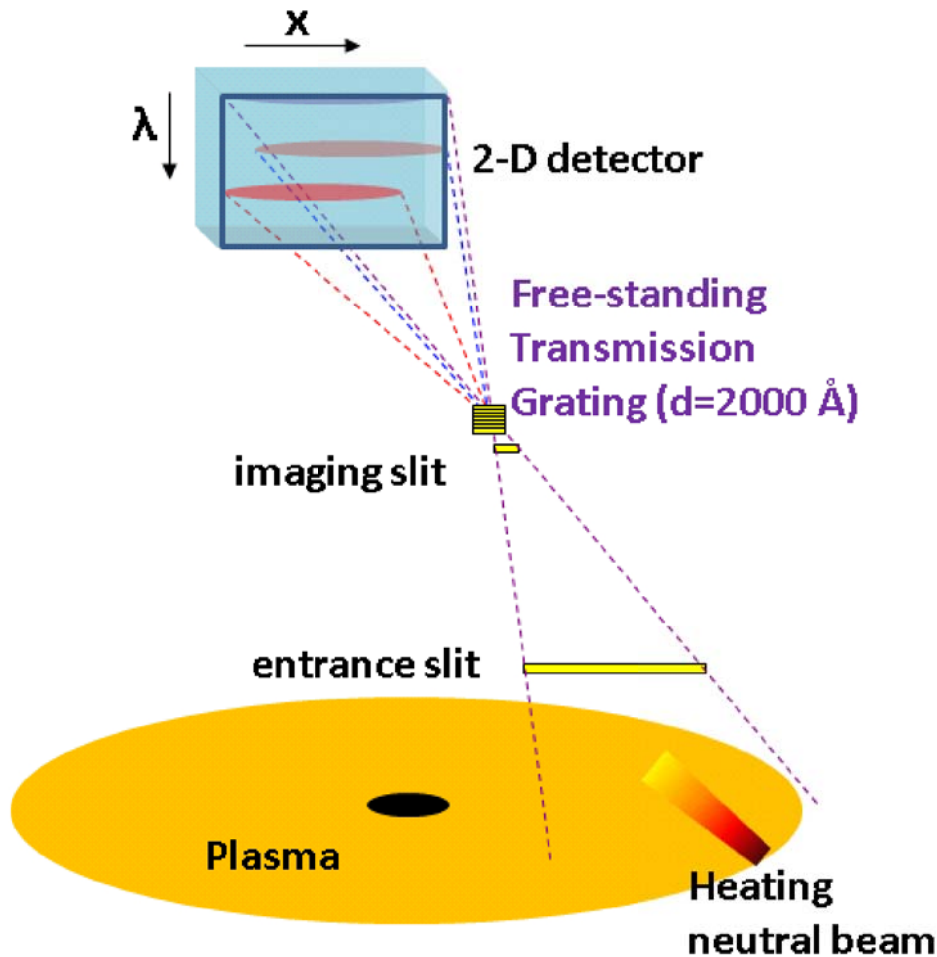
- Thin filters have increasing difficulty at higher core T_e
overestimates core $T_e \sim 20\%$



- Thicker filters needed for high T_e reconstruction

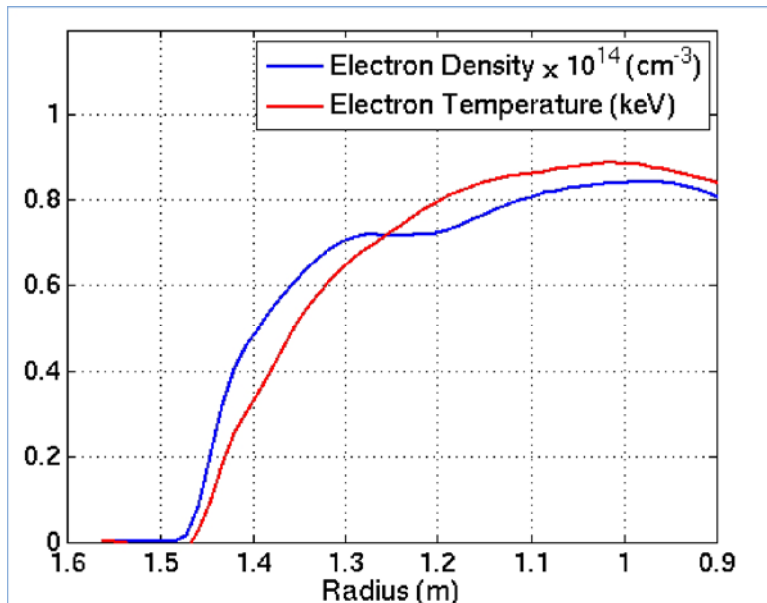
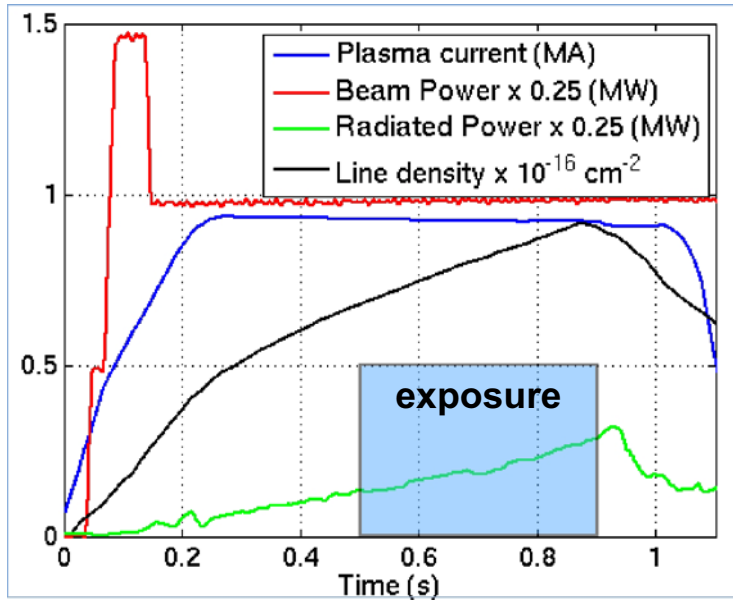
Transmission Grating Imaging Spectrometer provides radially resolved profiles of impurity line spectra

(see Stutman, Kumar this conference)



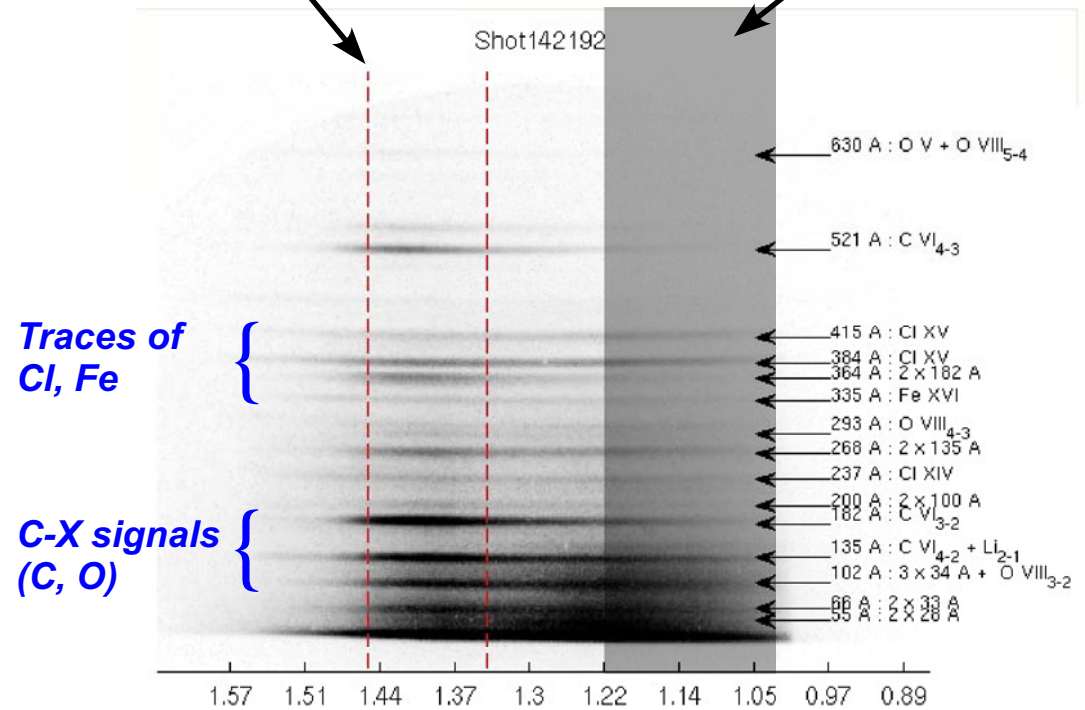
- Impurity profile information improves ME-SXR fast temperature reconstruction

TGIS measurements of standard NSTX H-mode plasmas show primarily low-Z impurities, C & O, with some Cl, Fe



Strong contributions from NBI C-X

Vignetted signal



- Previous modeling uses impurity concentrations consistent with measurements
- MPTS, TGIS measurements provide added information for ME-SXR fitting

Modeling for ME-SXR diagnostics demonstrates discrimination of fast T_e in addition to changes of impurities

- Linearized expansion model isolates dependence on T_e , n_e
 - careful selection of filter ratios can maximize T_e sensitivity
 - sensitivity to impurities can be minimized or maximized
 - collection of filters necessary to maintain sensitivity over range of plasma T_e and impurity content
- Fast impurity profile and electron temperature measurements will be used for (see Stutman):
 - high resolution edge/core impurity transport measurements
 - perturbative electron transport measurements (w/ laser blow-off)
- High spatial, time resolution at the edge will measure:
 - edge profile response to applied 3D fields
 - ELM precursor and lifecycle details
- Fast T_e reconstructions using multiple data sources and neural-network processing could provide robust, real-time measurements